

Effect of Prandtl Number on Natural Convection Heat Transfer from a Heated Semi-Circular Cylinder

Avinash Chandra and R. P. Chhabra*

Abstract—Natural convection heat transfer from a heated horizontal semi-circular cylinder (flat surface upward) has been investigated for the following ranges of conditions; Grashof number, and Prandtl number. The governing partial differential equations (continuity, Navier-Stokes and energy equations) have been solved numerically using a finite volume formulation. In addition, the role of the type of the thermal boundary condition imposed at cylinder surface, namely, constant wall temperature (CWT) and constant heat flux (CHF) are explored. Natural convection heat transfer from a heated horizontal semi-circular cylinder (flat surface upward) has been investigated for the following ranges of conditions; Grashof number, and Prandtl number. The governing partial differential equations (continuity, Navier-Stokes and energy equations) have been solved numerically using a finite volume formulation. In addition, the role of the type of the thermal boundary condition imposed at cylinder surface, namely, constant wall temperature (CWT) and constant heat flux (CHF) are explored. The resulting flow and temperature fields are visualized in terms of the streamline and isotherm patterns in the proximity of the cylinder. The flow remains attached to the cylinder surface over the range of conditions spanned here except that for and ; at these conditions, a separated flow region is observed when the condition of the constant wall temperature is prescribed on the surface of the cylinder. The heat transfer characteristics are analyzed in terms of the local and average Nusselt numbers. The maximum value of the local Nusselt number always occurs at the corner points whereas it is found to be minimum at the rear stagnation point on the flat surface. Overall, the average Nusselt number increases with Grashof number and/ or Prandtl number in accordance with the scaling considerations. The numerical results are used to develop simple correlations as functions of Grashof and Prandtl number thereby enabling the interpolation of the present numerical results for the intermediate values of the Prandtl or Grashof numbers for both thermal boundary conditions.

Keywords—Constant heat flux, Constant surface temperature, Grashof number, natural convection, Prandtl number, Semi-circular cylinder

I. INTRODUCTION

NATURAL convection from a heated cylindrical body immersed in quiescent fluids has been studied by numerous researchers. The heat transfer by natural convection always occurs whenever a temperature gradient is present in a field. In industrial practice, natural convection heat transfer occurs in natural draft cooling towers, heat exchangers, solar water heaters, etc. Much of the literature on natural convection, however, concerns the case of a circular cylinder

in various orientations such as horizontal, vertical or inclined. Owing to the space constraints and improved heat transfer/pressure drop characteristics, new and novel designs of heat exchangers employ tubes of non-circular cross-sections [1, 2]. Thus, for instance, semi-circular cylinders are encountered in the design of novel heat exchangers for the processing of heat sensitive materials such as pharmaceutical, personal care products, etc. Additional examples of heat transfer from a semi-circular cylinder are found in thermal processing of food, sub-sea vessels, flow dividers used in polymer processing to form weld lines, cooling of electronics components, compact heat exchangers, etc. In addition, natural convection heat transfer is strongly influenced by the shape and orientation of the bluff body. For instance, for a bluff body with a flat surface oriented transverse to the gravity, there is no component of the gravity along such a flat surface and therefore, heat transfer can only occur by conduction. The case of a semi-circular cylinder can thus provide useful physical insights.

In spite of its pragmatic and fundamental significance, momentum and heat transfer characteristics of a semi-circular cylinder have received only scant attention. While the voluminous literature concerning the single and multiple circular cylinders has been thoroughly reviewed in excellent books and review papers [3-8], the corresponding limited literature for square, elliptical, triangular, semi-circular cylinders has been summarized in some recent studies [9-20]. In particular, the scant results for a semi-circular cylinder have been reviewed in our previous studies [17-21]. In addition, the relevant studies are briefly summarized here. Based on the laminar boundary layer approximation, [22] proposed a correlation for the natural convection heat transfer from a heated horizontal circular cylinder under the CHF condition. Subsequently, they [23] extended this work to the turbulent free convection regime. [24] reported an experimental and numerical investigation of natural convection from a circular cylinder for the Rayleigh number range of $74 < Ra < 3400$ under the CWT boundary condition. Their experimental and numerical values were found to be within $\pm 20\%$ error band and the possible reasons for such large discrepancies have been advanced. [9] illustrated the role of the two thermal boundary conditions, namely, constant temperature (CWT) and constant heat flux (CHF) on the natural convection from a tilted square cylinder placed in a square enclosure. There has been only one experimental study [16] on free convection from a semi-circular cylinder to air ($Pr = 0.7$). [16] imposed the constant heat flux condition on the surface of the semi-circular cylinder for three orientations of the semi-circular

Prof. R. P. Chhabra is with Department of Chemical Engineering, Indian Institute of Technology Kanpur, India (*corresponding author, phone: +91-512-2597393; Fax: 00 91 512 2590104; e-mail: chhabra@iitk.ac.in).

Avinash Chandra, a Ph.D. student in Department of Chemical Engineering, Indian Institute of Technology Kanpur, India .e-mail: avich@iitk.ac.in

cylinder, the flat base facing downward, upward and along the direction of gravity. Predictive correlations have been proposed by them in terms of Rayleigh number, inclination angle and orientation angle of the semi-circular cylinder to predict the average Nusselt number for wide ranging values of Grashof number as $1.5 \times 10^3 \leq Gr \leq 8.5 \times 10^6$ and the overall heat transfer was found to be minimum for the case when the flat surface of the semi-circular cylinder was oriented downward. This is obviously due to the fact that there is no component of gravity along this horizontal direction. It is thus abundantly clear that little is known about the free convection heat transfer from a semi-circular cylinder.

In this work, new extensive numerical results elucidating the effects of Grashof number ($10 \leq Gr \leq 10^5$) and Prandtl number ($0.72 \leq Pr \leq 100$) on the detailed flow and heat transfer characteristics of a semi-circular cylinder immersed in stagnant fluids with its flat surface oriented upward are reported. Furthermore, the influence of the two commonly employed boundary conditions, *i.e.*, constant wall temperature (CWT) or constant heat flux (CHF), on the surface of the cylinder is also investigated.

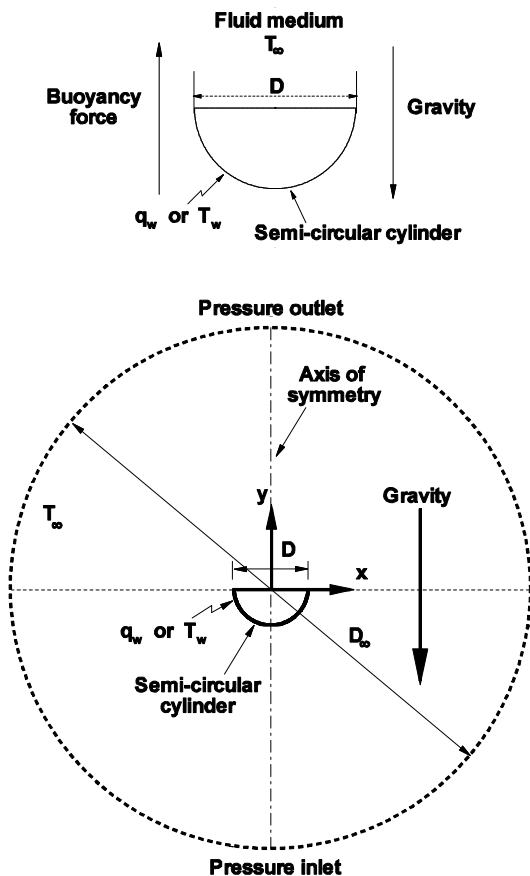


Fig. 1 Schematic representation of the physical model and computational domain

II. PROBLEM STATEMENT AND MATHEMATICAL FORMULATION

Consider the two dimensional ($2-D$) semi-circular cylinder of diameter, D (infinitely long in z -direction) immersed in a stagnant fluid at temperature, T_∞ . The flat surface of the cylinder is oriented upward in the positive y -direction, as shown in Fig. 1. While the actual boundary conditions on the surface of the cylinder can be quite complex, the two commonly used idealizations, namely constant wall temperature (CWT) and constant heat flux (CHF), are employed in this work. The semi-circular cylinder is concentrically placed in an artificial sufficiently large circular domain (in order to minimize the boundary effect) of diameter, D_∞ to approximate the unconfined flow condition. Except the fluid density, the other thermo-physical properties (*e.g.*, viscosity, μ , thermal conductivity, k , heat capacity, c_p) of the fluid are assumed to be independent of temperature and the viscous dissipation effect in energy equation is also neglected for the present range of the Grashof number, Gr and Prandtl number, Pr . The standard *Boussinesq approximation* [$\rho = \rho_\infty (1 - \beta(T - T_\infty))$] is used to model the density variation with temperature and this effect is incorporated in the body force term in the y -component of the Navier-Stokes equations. The governing equations consisting of the continuity, Navier-Stokes and thermal energy equations are written in their dimensionless form as follows:

Continuity equation:

$$\frac{\partial U_x}{\partial x} + \frac{\partial U_y}{\partial y} = 0 \quad (1)$$

Navier-Stokes equations:

x -component

$$\frac{DU_x}{Dt} = -\frac{\partial p}{\partial x} + \frac{1}{\sqrt{Gr}} \nabla^2 U_x \quad (2)$$

y -component

$$\frac{DU_y}{Dt} = -\frac{\partial p}{\partial y} + \frac{1}{\sqrt{Gr}} \nabla^2 U_y + \theta \quad (3)$$

Thermal energy equation:

$$\frac{D\theta}{Dt} = \frac{1}{Pr\sqrt{Gr}} \nabla^2 \theta \quad (4)$$

Based on the information available for a circular cylinder [5], the flow is assumed to be laminar, steady, two-dimensional and symmetric about the y -axis for the ranges of conditions employed here, *i.e.*, Grashof number, $10 \leq Gr \leq 10^5$ and Prandtl number, $0.72 \leq Pr \leq 100$. Hence, the numerical solution of the governing equations is sought only for $x \geq 0$ thereby economizing on the computational effort. However, in a few cases, particularly at the maximum values of Grashof number and Prandtl number employed here, time-dependent equations have been solved to confirm that the flow

is indeed steady over the range of conditions encompassed here.

The physically realistic (non-dimensional) boundary conditions for this flow configuration are written as follows:

A. At the Inlet Boundary

The lower half of the computational domain ($y \leq 0$) is designated as the inlet. The “pressure inlet” boundary condition is imposed at the inlet boundary with zero input value of the total gauge pressure and the temperature is set equal to the faraway fluid temperature, *i.e.*, $\theta = 0$.

B. At the Surface of the Cylinder

The usual no-slip boundary condition is imposed for flow, *i.e.*

$$U_x = 0; \quad U_y = 0 \quad (5)$$

and the CWT or CHF condition is implemented for temperature as follows:

$$\begin{cases} \theta = 1 & \text{for CWT condition} \\ \frac{\partial \theta}{\partial n_s} = -1 & \text{for CHF condition} \end{cases} \quad (6)$$

Where n_s is the outward unit vector normal to the surface of the semi-circular cylinder.

C. At the Outer Boundary

The upper half ($y \geq 0$) of the computational domain is designated as the outlet. The “pressure outlet” boundary condition is applied at the exit boundary with the zero input value of the static gauge pressure and the temperature is set equal to the faraway fluid temperature, *i.e.*, $\theta = 0$. The influence of the other types of outer boundary conditions at the outer boundary has been discussed elsewhere [25].

D. At the Plane of Symmetry ($x = 0$)

Owing to the symmetry of the flow about the y -axis, the following boundary conditions are used on $x = 0$ plane:

$$U_x = 0; \quad \frac{\partial U_y}{\partial x} = 0; \quad \text{and} \quad \frac{\partial \theta}{\partial x} = 0 \quad (7)$$

The variables appearing in the preceding equations are rendered dimensionless using D , U_c , D/U_c and ρU_c^2 as scaling variables for length, velocity, time and pressure respectively. Whereas the non-dimensional temperature is defined here as follows for the CWT and CHF conditions:

$$\theta = \begin{cases} \frac{(T - T_\infty)}{(T_w - T_\infty)} & \text{for CWT condition} \\ \frac{(T - T_\infty)}{(q_w D/k)} & \text{for CHF condition} \end{cases} \quad (8)$$

Using simple dimensional considerations, the reference velocity, U_c for the natural convection heat transfer is defined as:

$$U_c = \sqrt{Dg\beta\Delta T} \quad (9)$$

and the characteristic temperature difference is given as $\Delta T = (T_w - T_\infty)$ for the CWT condition and $\Delta T = (q_w D/k)$ for the CHF condition.

Thus, the free convection heat transfer in Newtonian fluids is governed by the two dimensionless groups, *i.e.*, Grashof number and Prandtl number, which are defined as follows for the CWT and CHF conditions.

TABLE I
COMPARISON OF THE AVERAGE NUSSELT NUMBER WITH LITERATURE
VALUES UNDER CHF CONDITION FOR A CIRCULAR CYLINDER

$Gr.Pr$	Churchill and Chu [23]	Martynenko and Khramtsov [5]	Present
1.4×10^3	2.831	2.718	2.867
2.1×10^3	3.095	2.948	3.062
3.15×10^3	3.387	3.196	3.269
4.2×10^3	3.612	3.386	3.429
5.6×10^3	3.855	3.586	3.598
7×10^3	4.056	3.750	3.735
7×10^4	6.932	6.517	6.216
5×10^5	11.10	10.45	9.975
2.5×10^6	16.43	14.02	14.57
1×10^7	23.08	19.55	20.54

E. Grashof Number

The Grashof number represents the relative importance of the buoyancy force to viscous force. The role of the Grashof number in natural convection is similar to that of the Reynolds number in forced convection. Thus, the increasing value of Grashof number implies the increasing strength of the flow. It is defined here for the CWT and CHF conditions as:

$$Gr = \begin{cases} \left(\frac{\rho}{\mu}\right)^2 D^3 g \beta \Delta T & \text{for CWT condition} \\ \left(\frac{\rho}{\mu}\right)^2 D^4 g \beta \left(\frac{q_w}{k}\right) & \text{for CHF condition} \end{cases} \quad (10)$$

F. Prandtl Number

The Prandtl number is the ratio of the momentum diffusivity to thermal diffusivity and is defined as follows:

$$Pr = \frac{c_p \mu}{k} \quad (11)$$

The product of Grashof number and Prandtl number (Rayleigh number, $Ra = Gr.Pr$) is also used as another governing parameter, but only two out of the three (Gr , Pr and Ra) are independent.

G. Nusselt Number

The Nusselt number expresses the heat transfer coefficient in non-dimensional form. Naturally, it varies from one point to another on the surface of the cylinder. The local Nusselt number is defined as:

$$Nu = \frac{hD}{k} = \begin{cases} -\frac{\partial \theta}{\partial n_s} & \text{for CWT condition} \\ \frac{1}{\theta|_s} & \text{for CHF condition} \end{cases} \quad (12)$$

The average value of Nusselt number Nu_{avg} is calculated simply as:

$$Nu_{avg} = \frac{1}{S} \int_S Nu \, ds \quad (13)$$

Thus, for a given shape and orientation, the average value of Nusselt number, Nu_{avg} is solely a function of the Grashof number (Gr), Prandtl number (Pr) and the imposed thermal boundary conditions (CWT or CHF) at the cylinder surface. This work endeavors to establish this relationship.

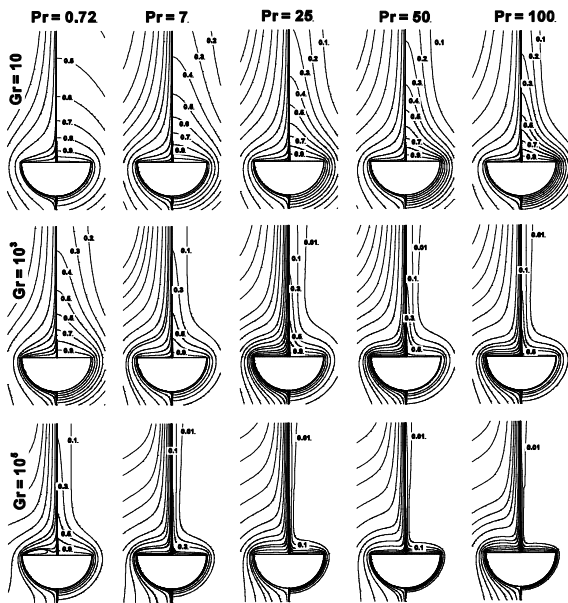


Fig. 2 Typical isotherm (right half) and streamline (left half) profiles for the CWT condition

III. NUMERICAL METHODOLOGY AND CHOICE OF COMPUTATIONAL PARAMETERS

The numerical solution of the continuity, Navier-Stokes and thermal energy equations (Eq. (1)-(4)) along with the prescribed boundary conditions is obtained using the finite volume based solver FLUENT (version 12.1). The physical problem is meshed using a large number of unstructured quadrilateral cells and the grid is made sufficiently fine adjacent to the semi-circular cylinder, in order to capture the steep velocity and temperature gradients in this region. The two-dimensional, laminar, steady, coupled solver is used to

solve the governing equations along with the prescribed boundary conditions. As noted earlier, to ascertain the nature of the flow regime and to circumvent the convergence problems, the solution is initiated using the unsteady solver, the value of drag is monitored until it is stabilized, then we switch to the steady solver. The absolute convergence criterion of 10^{-7} for continuity, x -momentum, y -momentum and that of 10^{-12} for energy equations have been this work. More detailed discussions regarding the domain and grid selection can be found elsewhere [20], suffice it to say here that the results reported herein are based on the following optimum choices: $D_-/D = 600$ and a grid with $\delta/D = 0.005$, $N_r = 258$, $N = 51340$. Furthermore, for the time integration, an adaptive time step procedure is adopted here, akin to that employed elsewhere [20].

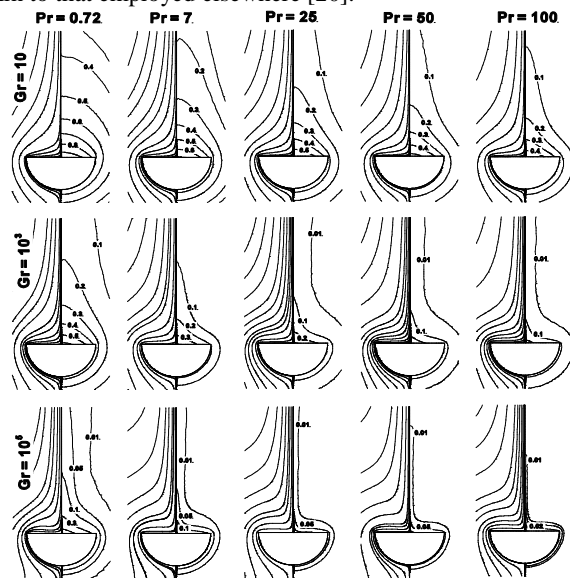


Fig. 3 Typical isotherm (right half) and streamline (left half) profiles for the CHF condition

IV. RESULTS AND DISCUSSION

The methodology used in this study has been extensively validated for forced convection [17, 18], mixed convection [19] and free convection heat transfer [20] from a heated semi-circular cylinder with constant wall temperature. In addition, for a circular cylinder, the present values of the average Nusselt number Nu_{avg} are compared with the literature values [5, 23] in Table I for the CHF condition. The present results are seen to differ by up to 5% from that of Martynenko and Khramtsov [5]. While the match with the approximate treatment of Churchill and Chu [23] is less good but the deviation increases with Rayleigh number, Ra .

Based on our past experience and on the validation reported elsewhere [20] together with the results shown in Table I here, the new results on natural convection heat transfer from a heated semi-circular cylinder are believed to be reliable within $\pm 5\%$.

A. Streamlines and isotherm profiles

Usually, the structure of the flow and temperature fields is visualized in terms of the streamline and isotherm contours. Representative streamline (left half) and isotherm (right half) contours are shown in Figs. 2 and 3 for a range of values of Gr and Pr , and for the CWT and CHF conditions respectively. A steady upward current is set up along the curved surface of the semi-circular cylinder due to the density gradient present in the vicinity of the cylinder. A plume formation is seen causing the fluid motion in the upward direction. Irrespective of the type of the boundary condition, the plume size reduces with the increasing values of the Grashof and/or Prandtl number. A separation bubble is seen only in one case corresponding to that of CWT condition at $Gr = 10^5$ and $Pr = 0.72$ (Fig. 2). It is presumably so due to the fact that at high Grashof numbers, a fluid element will not be able to negotiate the sudden change in the direction due to the loss of curvature at the corner thereby leading to flow separation at the rear flat surface, which is suppressed by the increasing Prandtl number (Pr) due to the gradual thinning of the boundary layer. This can also be interpreted in terms of the inverse dependence of the Grashof and Prandtl numbers on the momentum diffusivity. The clustering of streamlines and isotherms at the cylinder surface is more intense for the CHF condition than that for the CWT condition. All else being equal, the plume is seen to be larger under the CWT condition than that for the CHF condition.

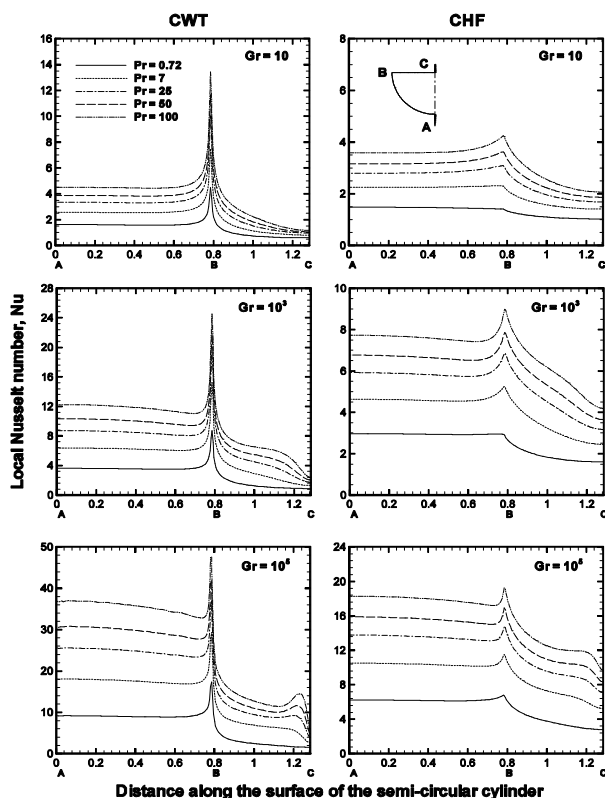


Fig. 4 Effect of Grashof number, Gr and Prandtl number, Pr on local Nusselt number, Nu on the surface of the semi-circular cylinder

B. Local Nusselt number

Fig. 4 shows representative results highlighting the influence of both Grashof and Prandtl numbers and the CWT and CHF conditions on the spatial variation of the local Nusselt number (Nu) on the surface of the semi-circular cylinder. In both cases, qualitatively similar trends are over the present range of conditions. The maximum and minimum values of the local Nusselt number (Nu) occur at the corner point B and at the rear stagnation point C respectively for all cases irrespective of the type of the thermal boundary condition (CWT or CHF) at the cylinder surface. This is due to the sudden bending of the streamlines and isotherms at the corner point B, the thermal boundary layer becomes thin and facilitates heat transfer at the corner point B whereas at the rear stagnation point C, the fluid is almost stagnant because of the fact that there is no component of gravity in the x -direction. The local Nusselt number (Nu) increases with the Grashof number (Gr) and Prandtl number (Pr) at each point on the surface of the cylinder. This is simply so due to the progressive thinning of the thermal boundary layer. Further examination of Fig. 4 suggests that the Nusselt number, Nu for the CWT condition is more than the corresponding values for the CHF condition and this difference increases with Rayleigh number (Ra). This is qualitatively in line with the trend observed by De and Dalal [9] for the case of the tilted square cylinder. At the front stagnation point (point A), the functional dependence of the Nusselt number on the Grashof number (Gr) and Prandtl number (Pr) is best represented by the following correlation:

$$Nu_0 = A + B (Pr^{0.27} Gr^{0.22}) \quad (14)$$

$$\text{Where, } A = \begin{cases} 0.43 & \text{for CWT} \\ 0.78 & \text{for CHF} \end{cases} \quad \text{and } B = \begin{cases} 0.77 & \text{for CWT} \\ 0.46 & \text{for CHF} \end{cases}$$

Eq. (14) correlates the present numerical values of the local Nusselt number, Nu_0 at the front stagnation point A with the average and maximum error of 3.4% and 8.7% respectively for the CWT condition whereas for the CHF condition, the average and maximum deviations are 5.2% and 14% respectively. The parity plot between the actual numerical values and the predictions of Eq. (14) is shown in Fig. 5.

C. Average Nusselt number

The average value of the heat transfer coefficient is often needed in process engineering and design applications. The influence of the Grashof number and Prandtl number on the average Nusselt number (Nu_{avg}) is shown in Fig. 6 for the CWT and CHF conditions. The average value of the Nusselt number (Nu_{avg}) increases with Grashof and Prandtl numbers in both cases. Broadly, as the value of the Rayleigh number (Ra) increases, advection becomes stronger and thus heat transfer increases. This trend is qualitatively consistent with

that seen in the forced convection [17], mixed convection [19] and free convection [20] regimes for a semi-circular cylinder, as well as for bluff bodies of other shapes [10, 25]. Following the approach employed in our recent studies [17, 18, 20], the present numerical results are correlated reasonably well by the following relationship.

$$Nu_{avg} = 0.78 Pr^a Gr^b \quad (15)$$

$$\text{Where, } a = \begin{cases} 0.27 & \text{for CWT} \\ 0.21 & \text{for CHF} \end{cases} \text{ and } b = \begin{cases} 0.2 & \text{for CWT} \\ 0.18 & \text{for CHF} \end{cases}$$

Eq. (15) correlates the numerical values of the average Nusselt number (Nu_{avg}) with an average error of 5.4% and 3.7% for the CWT and CHF conditions respectively, which reaches the maximum value of 17% for both cases. Fig. 5 shows the parity plot between the actual numerical values and the predictions of Eq. (15).

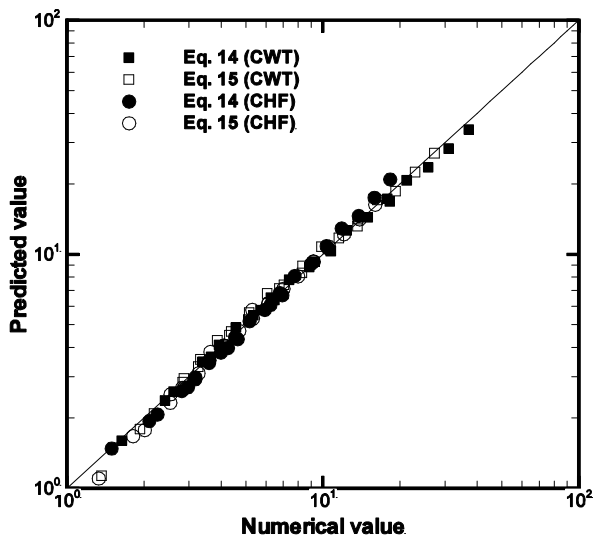


Fig. 5 Parity plot between the present results and the predicted values using Eq. (14) and Eq. (15): \square for CWT and \circ for CHF

V. CONCLUSIONS

Extensive numerical results for the laminar natural convection heat transfer from a heated semi-circular cylinder are obtained for the range of conditions as: Grashof number, $10 \leq Gr \leq 10^5$ and Prandtl number, $0.72 \leq Pr \leq 100$. The role of the thermal boundary conditions, namely, constant wall temperature (CWT) and constant heat flux (CHF) on the cylinder surface has also been illustrated. The flow and temperature fields are depicted in terms of streamline and isotherm patterns. Overall, the flow remains attached to the cylinder surface except in the case of $Gr = 10^5$ and $Pr = 0.72$ for the CWT condition. Irrespective of the type of thermal boundary condition, the maximum and minimum values of the local Nusselt number are occur at points B and C, respectively. The surface averaged Nusselt number shows a positive dependence on both Grashof number (Gr) and

Prandtl number (Pr). Furthermore, all else being equal, the values of average Nusselt number are seen to be greater in the case of CWT condition than that for the CHF condition. Simple predictive correlations have been developed for estimating the value of the Nusselt number at the front stagnation point and of the overall mean Nusselt number for given values of the Grashof and Prandtl numbers in a new application.

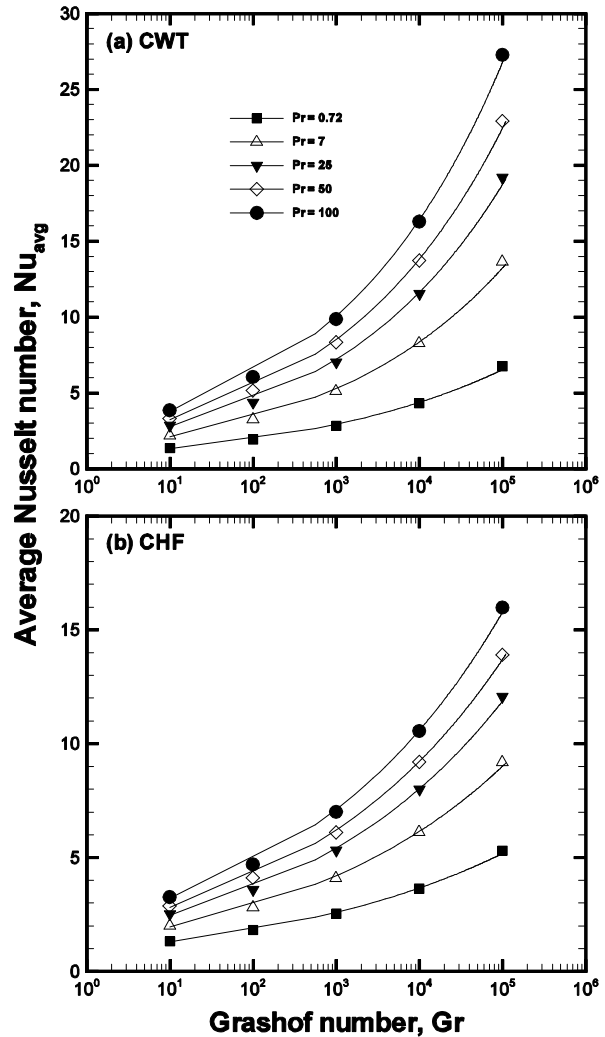


Fig. 6 Influence of Grashof number, Gr and Prandtl number, Pr on average Nusselt number, Nu_{avg} (a) CWT condition (b) CHF condition

NOMENCLATURE

- c_p specific heat of fluid ($J / kg.K$)
- D diameter of cylinder (m)
- D_∞ diameter of computational domain (m)
- Gr Grashof number (dimensionless)

- h heat transfer coefficient ($W / m^2.K$)
- k thermal conductivity of fluid ($W / m.K$)
- n_s unit vector normal to the surface of the cylinder
- N total number of cells in the computational domain
- N_p number of points on the surface of the semi-circular cylinder
- Nu local Nusselt number (dimensionless)
- Nu_0 local Nusselt number at the front stagnation point A (dimensionless)
- Nu_{avg} average Nusselt number (dimensionless)
- p pressure (dimensionless)
- Pr Prandtl number $[= c_p \mu / k]$ (dimensionless)
- Ra Rayleigh number $[= Gr.Pr]$ (dimensionless)
- q_w heat flux on the surface of the cylinder (W / m^2)
- S surface area (m^2)
- T fluid temperature (K)
- T_w temperature at the surface of the semi-circular cylinder (K)
- T_∞ fluid temperature far away from the cylinder (K)
- U_c reference velocity induced by buoyancy effect (m / s)
- U_x x-component of the velocity (dimensionless)
- U_y y-component of the velocity (dimensionless)

Greek symbols

- β coefficient of volumetric thermal expansion
- $$\left[= -\frac{1}{\rho} \frac{\partial \rho}{\partial T} \right]_T (K^{-1})$$
- δ grid spacing in the vicinity of the cylinder (m)
- θ fluid temperature $[= (T - T_\infty) / (T_w - T_\infty)]$ (dimensionless)
- μ viscosity of fluid ($Pa.s$)
- ρ density of fluid (kg / m^3)
- ρ_∞ density of fluid at the reference temperature T_∞ (kg / m^3)

Subscripts

- i, j, x, y Cartesian coordinates

Abbreviations

- CWT constant wall temperature
- CHF constant heat flux

REFERENCES

- [1] J. E. Hesselgreaves, Compact Heat Exchangers: Selection, Design and Operation, Pergamon, Oxford, 2001.
- [2] S. Kakac and H. Liu, Heat Exchangers: Selection, Rating, and Thermal Design, Second ed., CRC Press, Boca Raton, FL, 2002.
- [3] M. M. Zdravkovich, Flow Around Circular Cylinders, Volume 1: Fundamentals, Oxford University Press, New York, 1997.
- [4] M. M. Zdravkovich, Flow Around Circular Cylinders, Volume 2: Applications, Oxford University Press, New York, 2003.
- [5] O. G. Martynenko and P. P. Khramstov, Free Convective Heat Transfer, Springer, New York, 2005.
- [6] F. Kreith, The CRC Handbook of Thermal Engineering, CRC Press, Boca Raton, FL, 2000.
- [7] V. T. Morgan, The overall convective heat transfer from smooth circular cylinders, Advances in Heat Transfer 11 (1975) 199-264.
- [8] M. Coutanceau and J. R. Defaye, Circular cylinder wake configurations: A flow visualization survey, Applied Mechanics Reviews 44 (1991) 255-305.
- [9] A. K. De and A. Dalal, A numerical study of natural convection around a square, horizontal, heated cylinder placed in an enclosure, International Journal of Heat and Mass Transfer 49 (2006) 4608-4623.
- [10] C. Sasmal and R. P. Chhabra, Laminar natural convection from a heated square cylinder immersed in power-law fluids, Journal of Non-Newtonian Fluid Mechanics 166 (2011) 811-830.
- [11] A. O. Elsayed, E. Z. Ibrahim and S. A. Elsayed, Free convection from a constant heat flux elliptic tube, Energy Conversion and Management 44 (2003) 2445-2453.
- [12] R. P. Bharti, P. Sivakumar and R. P. Chhabra, Forced convection heat transfer from an elliptical cylinder to power-law fluids, International Journal of Heat and Mass Transfer 51 (2008) 1838-1853.
- [13] A. K. De and A. Dalal, Numerical study of laminar forced convection fluid flow and heat transfer from a triangular cylinder placed in a channel, Journal of Heat Transfer 129 (2007) 646-656.
- [14] A. Prhashanna, A. K. Sahu and R. P. Chhabra, Flow of power-law fluids past an equilateral triangular cylinder: Momentum and heat transfer characteristics, International Journal of Thermal Sciences 50 (2011) 2027-2041.
- [15] S. A. Nada, H. El-Batsh and M. Moawad, Heat transfer and fluid flow around semi-circular tube in cross flow at different orientations, Heat and Mass Transfer 43 (2007) 1157-1169.
- [16] S. A. Nada and M. Mowad, Free convection from a vertical and inclined semicircular cylinder at different orientations, Alexandria Engineering Journal 42 (2003) 273-283.
- [17] A. Chandra and R. P. Chhabra, Flow over and forced convection heat transfer in Newtonian fluids from a semi-circular cylinder, International Journal of Heat and Mass Transfer 54 (2011) 225-241.
- [18] A. Chandra and R. P. Chhabra, Momentum and heat transfer characteristics of a semi-circular cylinder immersed in power-law fluids in the steady flow regime, International Journal of Heat and Mass Transfer 54 (2011) 2734-2750.
- [19] A. Chandra and R. P. Chhabra, Mixed convection from a heated semi-circular cylinder to power-law fluids in the steady flow regime, International Journal of Heat and Mass Transfer (2011) In press.
- [20] A. Chandra and R. P. Chhabra, Laminar free convection from a horizontal semi-circular cylinder to power-law fluids, Submitted for publication (2011).
- [21] A. Chandra and R. P. Chhabra, Influence of power-law index on transitional Reynolds numbers for flow over a semi-circular cylinder, Applied Mathematical Modelling 35 (2011) 5766-5785.
- [22] S. W. Churchill, Laminar free convection from a horizontal cylinder with a uniform heat flux density, Letters in Heat and Mass Transfer 1 (1974) 109-112.
- [23] S. W. Churchill and H. H. S. Chu, Correlating equations for laminar and turbulent free convection from a horizontal cylinder, international Journal of Heat and Mass Transfer 18 (1975) 1049-1053.
- [24] S. O. Atayilmaz and I. Teke, Experimental and numerical study of the natural convection from a heated horizontal cylinder, International Communications in Heat and Mass Transfer 36 (2009) 731-738.
- [25] A. Prhashanna and R. P. Chhabra, Laminar natural convection from a horizontal cylinder in power-law fluids, Industrial and Engineering Chemistry Research 50 (2011) 2424-2440.